Multi-function Based Modeling of 3D Heterogeneous Wound Scaffolds for Improved Wound Healing

Ibrahim T. Ozbolat[1] and Bahattin Koc[2]

[1]University at Buffalo, iozbolat@buffalo.edu
[2]Sabanci University, University at Buffalo, bahattinkoc@sabanciuniv.edu

ABSTRACT

This paper presents a new multi-function based modeling of 3D heterogeneous porous wound scaffolds to improve wound healing process for complex deep acute or chronic wounds. An imaging-based approach is developed to extract 3D wound geometry and recognize wound features. Linear healing fashion of the wound margin towards the wound center is mimicked. Blending process is thus applied to the extracted geometry to partition the scaffold into a number of uniformly gradient healing regions. Computer models of 3D engineered porous wound scaffolds are then developed for solid freeform modeling and fabrication. Spatial variation over biomaterial and loaded bio-molecule concentration is developed based on wound healing requirements. Release of bio-molecules over the uniform healing regions is controlled by varying their amount and entrapping biomaterial concentration. Thus, localized controlled release is developed to improve wound healing. A prototype multi-syringe single nozzle deposition system is used to fabricate a sample scaffold. Proposed methodology is implemented and illustrative examples are presented in this paper.

Keywords: wound healing, wound healing scaffolds, multifunction-based modeling.
DOI: 10.3722/cadaps.2011.43-57

1 INTRODUCTION & LITERATURE REVIEW

Skin is the largest organ in human body and loss of integrity of skin due to injuries or illness may bring serious disabilities or even death. Causes of significant skin loss are thermal injuries, traumas and chronic ulcerations [29]. Wound healing in human skin is a familiar, everyday process however the underlying biology brings a very complex but orderly serious of events [48]. Due to possible lack of synchrony in the order of healing process, a wound behaves as a chronic wound that may even fail to heal. The ultimate goal of wound healing scaffolds is then to eliminate abnormalities that lead to impaired or slow healing. One common way is to prepare the wound bed to get the wound behave as normal i.e. surgical debridement [29].

Despite extensive research, wound healing remains partially understood. Human skin serves as a protective barrier against the environment and is composed of two layers: keratinized stratified outer layer (epidermis) and collagen-rich inner layer (dermis) [37]. Serious injuries or illnesses damage the

epidermis and sometimes even penetrates through the dermis. Wound contraction and matrix remodeling occur in the dermis in parallel with epidermal cell migration and proliferation during deep wound healing. Although the exact mechanism is still not clear, migration and proliferation of epithelial cells may be triggered by the absence of neighboring cells at the wound margin know as "free-edge effect" [29]. In the literature, wound healing of mammalian skins has been analyzed both experimentally and theoretically [6, 32, 39, 46, 52]. Several mathematical models have been proposed concentrating specifically upon the mechanism involved in epidermal healing. However, 3-D healing modeling of deep wounds and closure has not been investigated, and majority of research has been done by assuming a 1-D or 2-D healing process. Wound closure is indeed the centripetal movement process of the wound periphery and adjacent uninjured skin toward the wound center [47]. The healing of convex wound shapes follows a linear relationship between area and perimeter while the distance from the wound perimeter to any given point within the wound surface is always definable via a linear distance [6]. Moreover, several imaging techniques such as Laser Doppler Imaging [27], noninvestment tools with magnetic resonance imaging (MRI) [20] and 3D active contour segmentation [54] are used to capture wound geometry during healing process, and predict wound healing based on geometry, area and appearance [5, 19, 21, 30].

Fig. 1: A typical wound scaffold impregnated with cells, growth factors and proteins [29]. Courtesy of Elsevier.

A typical 3D wound scaffold, shown in Fig. 1, should posses several functions such as protecting wound from the external environment to prevent trauma, bacterial invasion and contact with caustic substances, and enabling oxygen transmit to wound surface . An appropriate oxygen balance should be maintained for optimal wound healing to support cell migration and mitosis [31]. Thus, semipermeable porous scaffolds are needed for dressing to create the optimal oxygen tension for accelerated wound healing. Although several single layer porous wound scaffolds have been applied in wound healing applications [18, 49], full thickness wounds involve the loss of epidermis and dermis layer of the skin that necessitates multilayered wound scaffolds . Bilayered structures reinforced with epidermal cells, collagen, human skin fibroblast and keratinocyte [3, 11, 17] have been successfully used in surgical wounds and ulcers compared to the standard therapies [13].

Biomaterials have been extensively used in medical applications. Alginates have been widely applied as hydrogel synthetic extracellular matrices (ECMs) for cell immobilization, cell transplantation and tissue engineering due to their physical properties that are similar to natural tissues [41]. Due to their gelatin property during in contact with body fluid, alginates have been one of the most popular biomaterials in wound care [1]. This property prevents the wound surface from drying out and provides a moist wound environment that leads a better repair of wound with less tissue loss from desiccation [53]. Besides, this eliminates fibre entrapment in the wound, which is a major cause of patient trauma during wound dressing removal [28]. Moreover, ionically crosslinked alginates release ions during in contact with body fluids that reduce bleeding during several surgical interventions [4]. Furthermore, alginates are highly absorbent (up to 15-20 times its own weight) and nonadherent that enables them to remain in wound bed for several days [31]. The quantity and quality of regenerating tissue depends on the present of biologic modifiers (i.e. growth factors and proteins), their activity with target cells and the extracellular matrix environment [23]. A wealth of growth factors such as epidermal growth factors (EGF), platelet-derived growth factor (PDGF), transforming growth factor-β (TGF-β), heparin binding epidermal growth factor (HB-EGF) and keratinocyte growth factor (KGF)

regulate wound healing [33]. Due to short biological half life, potential carcinogenesis risk and lack of tissue selectivity, proteins and growth factors needs to be controlled spatially and temporarily in a wound scaffold [40]. Changing incorporated bio-molecules and material concentrations provides a way to control release kinetics spatially. Multi-functional active wound scaffolds are hence needed to guide release kinetics spatially. Higher bio-molecule concentrations in specific sites result in higher amount of cumulative release. Material concentration however mediates release kinetic rate rather than changing cumulative release such as higher alginate concentration slows down release kinetics and vice versa [38].

Novel engineering approaches aims to develop more effective structures which are easy to handle, user friendly, acellular and impregnated with growth factors and proteins [29]. 3D customized porous scaffolds with localized based impregnation of cells, growth factors and proteins thus need to be considered for future trend in full thickness wound healing applications. This enables target delivery of loaded biological modifiers spatially i.e. gradient decrease in EGF through bottom sites of a wound scaffold while its effectiveness is disappearing in dermis.

The ultimate goal of this paper is to improve wound healing process in full thickness acute or chronic wounds by controlling release kinetics of bio-molecules spatially and temporarily to synchronize it with normal healing process. Thus, a new 3-D wound scaffold design is proposed to deliver bio-molecules locally and temporarily based on 3D wound healing needs. Wound scaffolds are thus developed and fabricated with spatially varying biomaterial and loaded bio-molecules concentration. A road map of proposed methodology is given in Fig. 2 beginning with processing wound images to extract the 3D wound scaffold geometry. 3D modeling of wound bed is then used to determine functionally gradient uniform regions based on linear healing of wound margin towards the wound center. Next, 3D model of porous wound scaffold for solid freeform fabrication (SFF) is generated with variational biomaterial and loaded bio-molecule concentration. Finally, toolpath of 3D model is generated and inputted into numerically controlled multi-syringe single nozzle solid freeform deposition system. The methodology is implemented and illustrative examples are given in this paper.

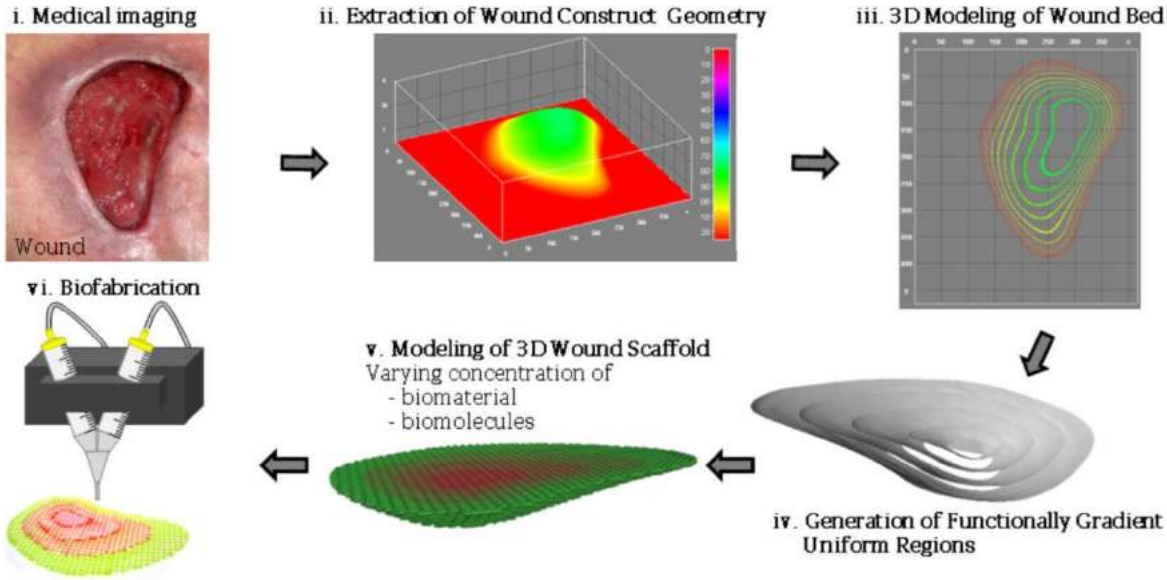

Fig 2: Road map of modeling and fabricating a wound scaffold with controlled material and loaded bio-molecule concentrations.

2 MULTIFUNCTION BASED VARIATIONAL MODELING OF 3D WOUND SCAFFOLDS

Wound healing can be enhanced by controlling localized protein and growth release over the scaffold. Adjusting the healing time of a specific region with respect to the release time of corresponding

growth factors or proteins would have a great impact on wound healing [40]. In this paper, proteins, growth factors and cells etc. are named with a general term of "bio-molecules". Release kinetics of bio-molecules can be temporarily controlled by controlling material and loaded bio-molecule distribution spatially in 3D. Material and bio-molecule distribution functions represent the concentration profile based on wound healing requirements. Concentration profile thus directs variation over the scaffold spatially. Three-dimensional geometry of customized scaffold is then formed by partitioning the scaffold into uniform regions with uniform existence of materials and bio-molecules. Discretization of the scaffold follows how a wound heals on human skin. In order to mimic 3-D wound healing process to partition the wound scaffold into uniform functional regions, concentration variation can be represented with relation to the 3D wound space boundaries or features. In this section, feature based representation of 3D wound scaffolds with multifunction based concentration profile is presented.

2.1 Feature-based Representation of 3D Wound Scaffolds

In feature-based representation, a 3D wound scaffold **S** is modeled as a collection of three characteristic sets [44]. Feature-based representation scheme is applied to represent **S** by combining concentration profile (**P**) with a set of features (**F**) and a set of geometric constraints (**C**) as follows:

$$S = (P, F, C) \tag{2.1}$$

$$P = \{f_m(u), f_b(u)\}$$

$$F = \{\{FF_i\}_{i=0,\ldots,n_i}, \{WF_j\}_{j=0,\ldots,m_j}\} \cap E^3$$

$$C = \{\{C_j\}_{j=0,\ldots,m_j}\}$$

Where E^3 is the three-dimensional Euclidean space. Concentration profile **P** guides concentration variation and is modeled as a free-form curve represented by B-spline functions of parametric distance u and degree (p). **P** comprises material concentration function $f_m(u)$ and loaded bio-molecule concentration function $f_b(u)$. Concentration property of **S** in this paper is thus directed by a multifunction driven concentration profile.

$$P = \sum_{i=0}^{e} N_{i,p}(u) Q_j \tag{2.2}$$

In Eqn (2.2), Q_j are the control points that control the concentration profile. Feature set **F** consist of form features $\{FF_i\}_{i=0,\ldots,m_i}$ and wound features $\{WF_j\}_{j=0,\ldots,m_j}$. Form features are geometric entities such as points, curves, surfaces or solid primitives that define the geometry of wound bed and hence the geometry of 3D porous scaffold. Wound features dominate the starting and ending points of concentration variation over the scaffold. Wound feature can be an arbitrary feature of 3D healing tissue space in the geometric form of a point, curve, surface or the entire boundary. Variation in material and bio-molecule concentration is confined by set of geometric constraints $\{C_j\}_{j=0,\ldots,m_j}$.

Geometric constraints limit concentration variation in a way that the concentration profile is not defined beyond the boundary of form features in the porous space of **S**. Feature-based representation of a sample 3D wound scaffold is demonstrated in Fig. 3. Wound scaffold (**S**) consists of 3 characteristics sets: set of features, set of geometric constraint and a multifunctional concentration profile. Feature set is a collection of 2 feature sets: a set of wound features and a set of form features. While wound healing process starts from the wound margin and proceeds towards the center of the wound (the point where wound converges), for illustrational purpose two wound features *WF*'s are defined over the wound geometry to mimic healing process: surface of wound bed (WF_1) and wound center (WF_2). Fig. 3 illustrates form features that represent the geometry of **S** including cylindrical solid primitives to model 3D porous shape for solid freeform fabrication (discussed in Section 2.3). Sample geometric constraints over form features are side surface and bottom surface of solid cylinder primitive. These are the boundaries that the concentration profile is not defined beyond (in void space). In Fig. 3, concentration variation is guided by the concentration profile **P**, with increasing material concentration function and decreasing impregnated bio-molecule concentration function

between 2 *WF*'s. Surface of wound bed defined as WF_1 can also be represented as a set of wound bed curves $\{I^k\}_{k=1,\ldots,K}$.

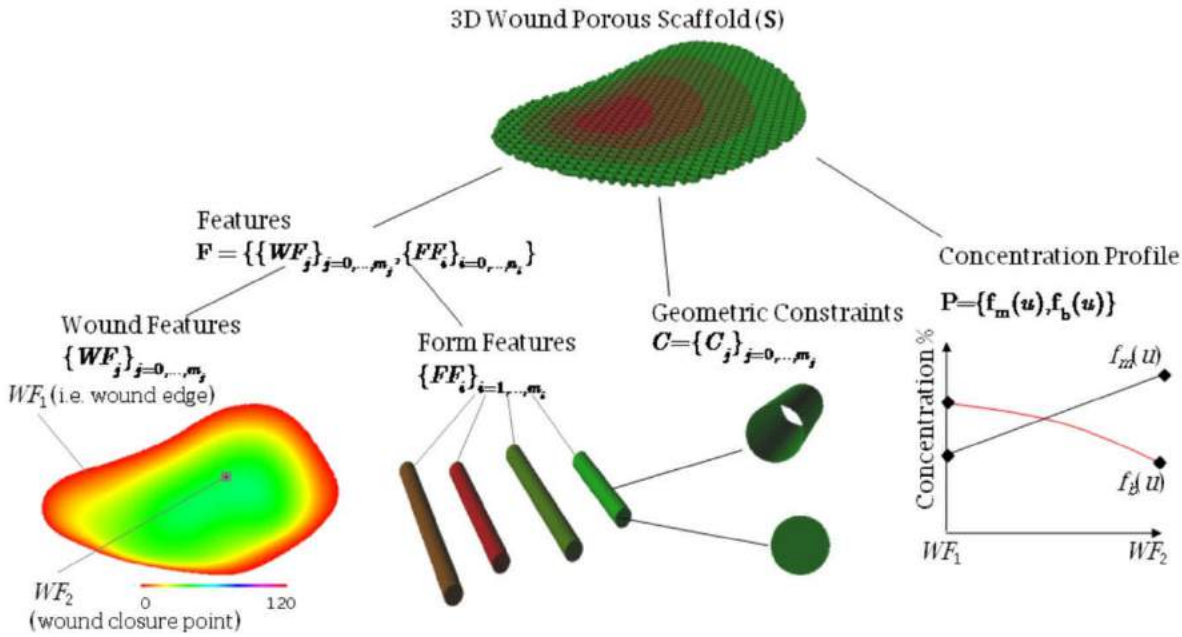

Fig 3: Feature-based representation of a sample wound scaffold.

It is assumed that the overall property Π^p including mechanical, functional and biological behavior of the wound scaffold is proportional to the concentration profile and is given in Eqn (2.3). Controlling concentration profile thus guides variation in mechanical, functional and biological properties through the scaffold to satisfy local requirements in healing wound (i.e. higher material concentration in certain sites improves mechanical properties and slows down the release of biologically active molecules).

$$\Pi^p \approx \mathrm{P} \tag{2.3}$$

2.2 Geometric Variational Model: Generation of Functionally Gradient Regions

Required bio-molecules can be delivered at a specific site over the wound space by synchronizing the delivery of controlled amount of bio-molecules with tissue regeneration. The geometry of a wound scaffold then needs to be varied based on wound surface movement to control improved and successful wound healing [24]. In the literature, 2-D wound healing progress has been studied to understand the contraction of wound margin through the wound center or the relation between wound perimeter with the wound area [6, 10, 16, 46-47]. However, all wounds have thickness and hence a 3-D geometry, and follow a 3-D healing process. Thus, a new 3-D blending operation is proposed to generate variation over the scaffold to mimic the linear healing process proposed in [6, 14-16, 22, 50-51]. Based on the above referred linear healing fashion, wound center (WF_2) where the wound closure converges and healing completes can be approximated as the projection of deepest point over wound top surface.

In this paper, a novel blending approach is developed for 3D modeling of heterogeneous wound scaffolds. Blending (also called skinning) is a process forming a surface between 2 *WF*'s that is a blend among a set of curves called sections curves denoted by $H_j^k(u)$, $j=1,\ldots,J$ (See our earlier work [36] for

details about blending). $H_j^k(u)$ is j^{th} section curve passing through I^k. Curve interpolation is performed across the equally distanced points of the section curves between 2 *WF*'s. Variation over the scaffold is represented by concentration profile that directs blending operation generating n number of blending curves (B_i^k). B_i^k represents the continuous variation on the geometry between two wound features. Blending curves are used to partition wound scaffolds into uniformly gradient healing regions. In order to generate n number of blending curves on the scaffold, discretization is performed on the concentration profile by dividing it into n-1 number of equivalent regions based on a parametric distance. In this paper, region generation is performed over 3-D geometry by applying blending process through set of $\{I^k\}_{k=1,\ldots,K}$ shown in Fig. 7(a). Each I^k generates J number of section curves $\{H_j^k(u)\}_{j=1,\ldots,J}$ illustrated in Fig. 7(b). Curve interpolation is performed across the equally distanced points of the section curves to generate n number of blending curves $\{B_i^k\}_{i=1,\ldots,n}$ shown in Fig. 7(c). In this work, surface generation discussed in our earlier study [45] is used to construct set of surfaces $\{S_i\}_{i=1,\ldots,n}$ (See Fig. 7(e)) from generated blending curves shown in Fig. 7(d).

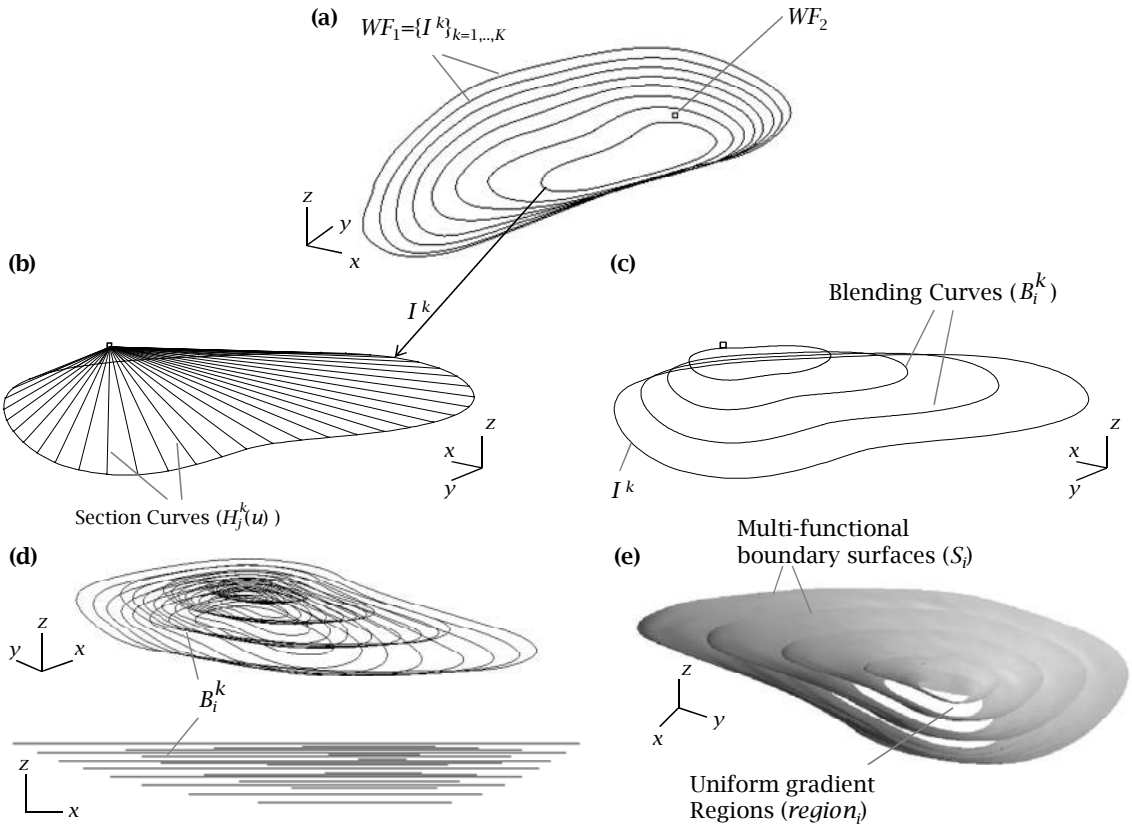

Fig. 4: Steps to obtain uniform regions: (a) Set of wound bed curves $\{I^k\}_{k=1,\ldots,K}$, (b) section curve generation, (c) applying blending process for each I^k, (d) generating blending curves and (d) obtaining multi-functional boundary surfaces (S_i).

The following algorithm is developed to generate uniform healing regions.

Algorithm I: Generation of uniform gradient regions
INPUT:
$\{WF_j\}_{j=0,\ldots,m_j}$: Set of wound features
$\{I^k\}_{k=1,\ldots,K}$: Set of wound bed curves
d : Dividing distance for section curve generation
n : Required number of uniform healing regions
OUPUT:
$\{S_i\}_{i=1,\ldots,n}$: Set of multi-functional boundary surfaces

START
$\forall I^k$:

Obtain the length of wound bed curve I^k (l^k) and number of section curves where $J = \frac{l^k}{d}$;

For ($j = 1$ to J) {
Generate section curve $H_j^k(u)$ from I^k to WF_2;
$j = j + 1$; } /*** End of 1st For Loop***/
For ($i = 2$ to n) {
Generate blending curve B_i^k through equally distanced points;
$i = i + 1$; } /*** End of 2rd For Loop***/
For ($i = 1$ to n) {
Generate multi-functional boundary surface S_i through set of blending curves $\{B_i^k\}_{k=1,\ldots,K}$;
$i = i + 1$; } /*** End of 3th For Loop***/

END

In this section, variation of scaffold geometry to localize material and entrapped bio-molecules is thus represented by a new 3-D blending operation generating n number of multi-functional boundary surfaces. This process is used to partition the entire geometry into uniform healing regions with identical properties. In the next section, development of porous wound scaffolds for solid freeform modeling and fabrication is presented.

2.3 3D Modeling for Solid Freeform Fabrication

Solid freeform fabrication (SFF) has been widely used for constructing tissue engineered scaffolds due to its high accuracy in micro-scale fabrication resolution [25, 43]. Applied SFF technology is recently utilized in drug metabolism studies and direct cell printing process for layer-by-layer dispensing of 3D alginate tissue scaffold [7-8]. In order to achieve truly interconnected internal architecture for cell growth and proliferation, the internal scaffold is formed by depositing cylindrical micro-filaments parallel to each other in every layer using a certain lay-down pattern. In this section, 3D modeling of heterogeneous wound scaffold is developed for SFF. Horizontal and vertical depositions are assumed to be positioned along *x*-axis and *y*-axis respectively.

The generated healing surfaces shown in Fig. 5(a) are sliced into a set of layers $\{L^s\}_{s=1,\ldots,S}$ generating set of contours $L^s = \{C_i^s\}_{i=1,\ldots,n}$ for layer-by-layer manufacturing shown in Fig. 5(b)-(c). For each L^s, filaments are generated with user defined filament diameter and distance between filaments. In Fig. 5(c), representation of toolpath generation on a sample layer for solid freeform modeling and fabrication is illustrated. Horizontal deposition over top layer L^1 is started with generating a number of equidistance horizontal lines l_{hor_j}. Then, a number of points $F_{hor_{j\,p}}^{\ s}$ are generated at the intersection

of each l_{hor_j} with each contour C_i^s, where $F_{hor_{jp}}^{\ s}$ is p^{th} point of j^{th} filament of L^s for horizontal deposition. Contour information for each $F_{hor_{jp}}^{\ s}$ is stored as $R_{hor_{jp}}^{\ s}$, where $R_{hor_{jp}}^{\ s}$ is the related contour information of point $F_{hor_{jp}}^{\ s}$. Thus, required information is kept to assign certain concentration values for cylindrical filaments between two consecutive points in i^{th} region ($region_i$).

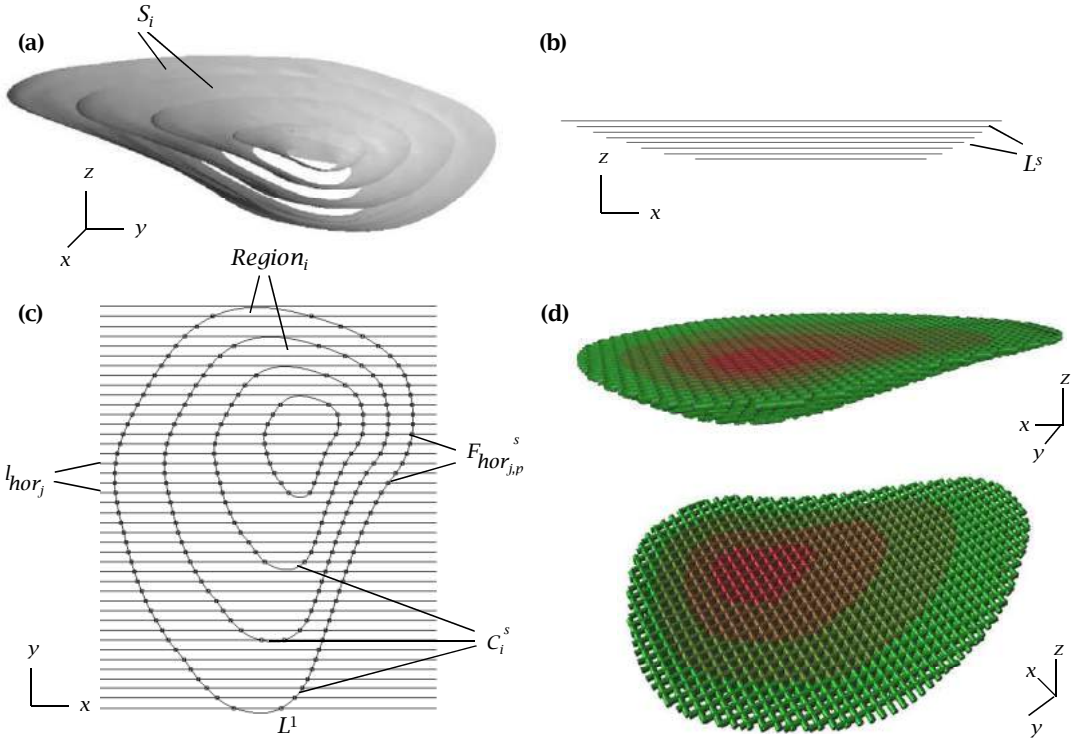

Fig. 5: 3D modeling of wound scaffolds for SFF systems (a) Set of multi-functional boundary surfaces $\{S_i\}_{i=1,\ldots,n}$ and (b) slicing all S_i's into set of layers $\{L^s\}_{s=1,\ldots,S}$. (c) Top layer L^1 is illustrated as a sample layer for toolpath generation, and (d) generated 3D wound scaffold model (Please see colored version).

The following algorithm is developed to generate points and corresponding contour information for toolpath development in solid freeform modeling and fabrication:

Algorithm II: Toolpath Generation
INPUT:

$\{S_i\}_{i=1,\ldots,n}$	:	Set of multi-functional boundary surfaces
Δl	:	Distance between filaments
h	:	Maximum depth of wound
d_f	:	Diameter of filament (also equal to the slicing thickness)

OUPUT:

$\{F_{hor_{jp}}^{\ s}\}_{s=1,\ldots,S;\ j=1,\ldots,J;\ p=1,\ldots,P}$	:	Set of points for horizontal filament deposition
$\{R_{hor_{jp}}^{\ s}\}_{s=1,\ldots,S;\ j=1,\ldots,J;\ p=1,\ldots,P}$	:	Set of contour information for generated set of points

START

Obtain number of layers $S=\frac{h}{d_f}+1$;

For (s=1 to S) {

Generate infinite horizontal plane G^s with z- coordinate $z=(s\text{-}1)d_f$;

For (i=1 to n) {

If ($G^s \cap S_i$ =! **NULL**) **Then** {

$C_i^s = G^s \cap S_i$; /***get contour when the plane intersects multi-functional boundary surface***/

} /***End of If-Statement***/

} /***End of 2nd For-loop***/

$L^s=\{C_i^s\}_{i=1,\ldots,n}$; /***define the layer as a set of contours with same z values***/

$s=s+1$; } /***End of 1st For-loop***/

$\forall L^s$:

j=1 ;

Add line l_{hor_j} from the top of L^s; /***Start adding horizontal line from the top***/

While ($L^s \cap l_{hor_j}$ =! **NULL**) {

p=1 ;

For (i=1 to n) {

While ($C_i^s \cap l_{hor_j}$ =! **NULL**) {

Get Point $F_{hor\,j\,p}^{\,s}$ as intersection of C_i^s and l_{hor_j} ;

Keep the contour information $R_{hor\,j\,p}^{\,s}$; /***keep information for region differentiation***/

$p=p+1$; } /***End of 2nd While-loop***/

} /***End of 3rd For-loop***/

$j=j+1$; /***Increment variable for the next line***/

$(l_{hor_j})_y=(l_{hor_j})_y+\Delta\, l$; /***Update the location of next line in $-y$ coordinate***/

Add line l_{hor_j} ; /***Add next horizontal line***/

} /***End of 1st While-loop***/

END

Similar algorithm can also be generated for point generation for vertical filament deposition. The generated set of points and contour information are used as inputs for the algorithm developed in our recent study [34] that generates 3D heterogeneous porous scaffolds with variational biomaterial and loaded bio-molecule concentration properties. In this section, modeling of geometric design for 3D wound scaffolds is developed for solid freeform fabrication systems. In the next section, implementation and illustrative examples are presented.

3 IMPLEMENTATION & EXAMPLES

Presented algorithms are implemented by developing a script in Rhinoceros 4.0 software [42] to generate 3D scaffolds in CAD with loaded bio-molecules. The dispersion of bio-molecules follows normal distribution over the cross-section of filaments. For details about stochastic distributions of bio-molecules in micro-filaments, the reader is referred to our earlier work [35]. In this paper, two images from pressure ulcer disease are processed for geometric modeling of wound scaffolds. Fig. 6(a) demonstrates a wound image from a recent study [2]. The image is then processed in ImageJ software and 3D wound scaffold geometry is extracted as in Fig. 10(c), which is the inverse of wound shape as illustrated in Fig. 6(b). Then, wound bed curves are generated for geometric modeling in CAD. By inputting the wound bed curves, 3D model of porous wound scaffold is developed based on a given

biomaterial and loaded bio-molecule concentration profile with a user defined number of regions for discretization purpose. In this work, it is assumed that the given concentration profiles follow tissue engineering and wound healing requirements. Fig. 7(a) illustrates the developed 3D model in CAD based on alginate and loaded microsphere concentration profile given in Fig. 7(b).

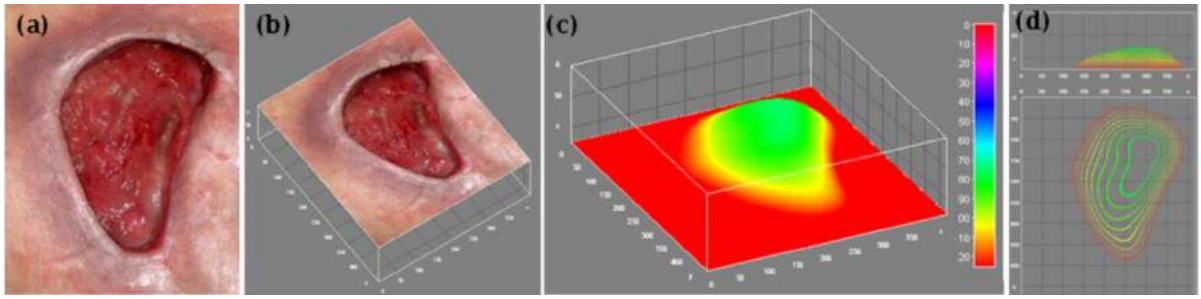

Fig. 6: Extraction of wound scaffold geometry: (a) wound images from recent study [2] is (b) processed in ImageJ software and (c) 3D geometry is extracted. Finally, (d) wound bed curves are generated for geometric modeling.

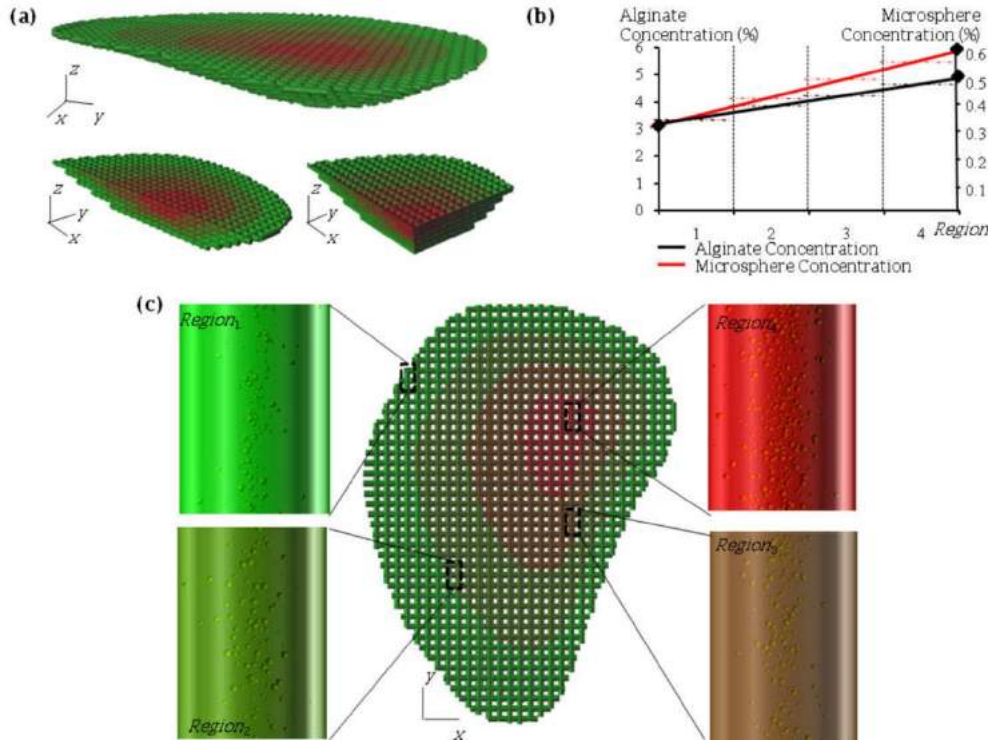

Fig. 7: Development of wound scaffold: (a) Generation of 3D model based on (b) concentration profile over 4 regions with (c) visualization of stochastic distribution of microspheres.

Variation in material concentration is characterized by color differentiation in RGB color space based on the following formula:

$$RGB_{i=1,\ldots,n}(r_i, g_i, b_i) = RGB_1 + \left(\frac{f_{m_i} - f_{m_1}}{f_{m_n} - f_{m_1}}\right)(RGB_n - RGB_1) \tag{2.4}$$

In Eqn (2.4), $RGB_i(r_i,g_i,b_i)$ is the assigned (red, green, blue) additive color value of i^{th} region ranges between colors of two extremes RGB_1 and RGB_n, $0 \le r_i,\ g_i,\ b_i \le 255$.

Based on the concentration profile given in Fig. 7(b), certain number of microspheres is distributed stochastically inside filaments in each region according to the quantification study performed in our earlier work [34]. Fig. 7(c) illustrates porous scaffold with highlighted differentiation in microsphere concentration between 0.3-0.6% (w/v).

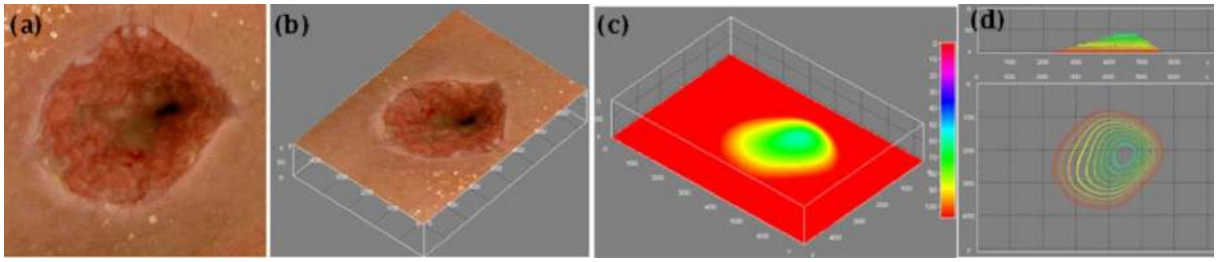

Fig. 8: Extraction of wound scaffold geometry: (a) wound images from recent study [12] is (b) processed in ImageJ software and (c) 3D geometry is extracted. Finally, (d) wound bed curves are generated for geometric modeling.

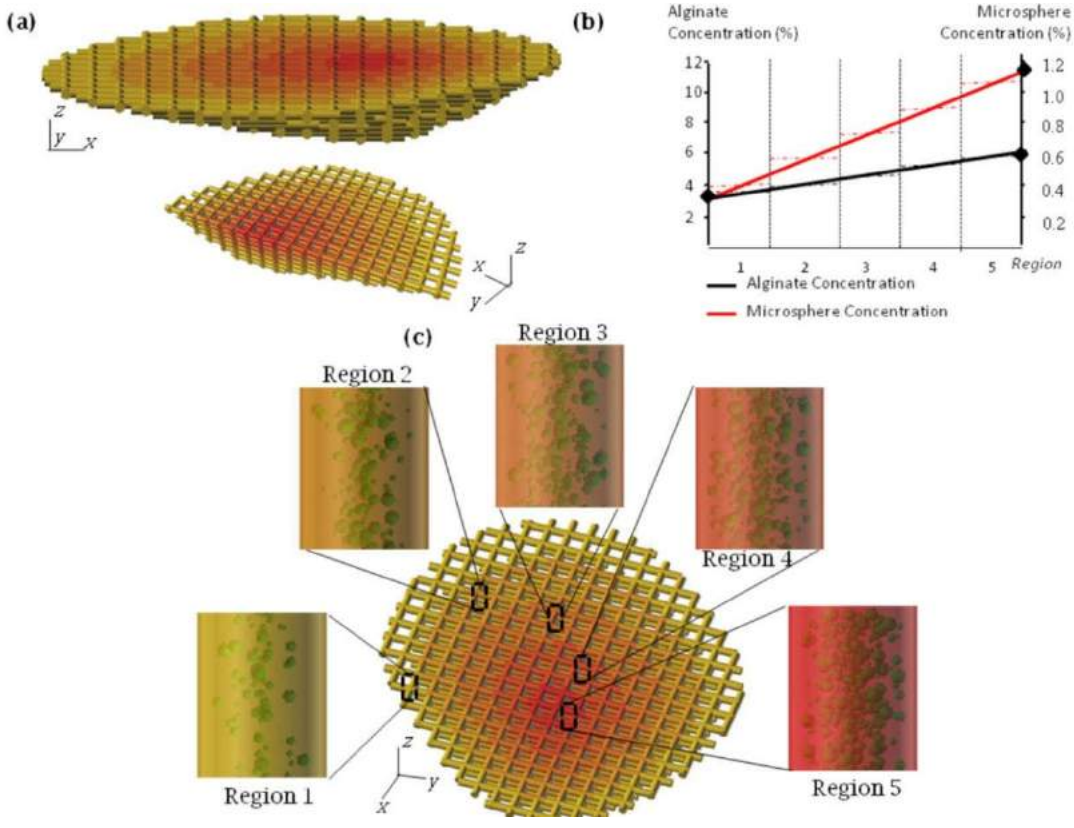

Fig. 9: Development of wound scaffold: (a) Generation of 3D model based on (b) varying alginate-microsphere concentration requirement over 5 regions with (c) visualization of stochastic distribution of microspheres.

Similar procedure is applied to another pressure ulcer wound image [12] (See Fig. 8(a)). After processing the image, 3D geometry is extracted in Fig. 8(c) and wound bed curves are generated (See Fig. 8(d)) for geometric modeling.

The wound scaffold is then developed based on the concentration profile demonstrated in Fig. 9(b). The wound scaffold is partitioned into 5 distinct regions with varying alginate concentration between 3-5% concentration with linearly increasing fashion through inner regions. Fig. 9(c) visualizes incorporated microspheres with increasing microsphere concentration between 0.3-1.1% spatially.

4 BIOFABRICATION

Biofabrication of sample wound scaffold is performed by a prototype multi-syringe single nozzle dispensing system shown in Fig. 10(a). The system runs in room temperature under low pressure (0-5 psi) to reduce fluidic shear forces that can damage incorporated bio-molecules or diminish their active properties. Mixing two different concentrations from each nozzle enables dispensing varying concentration of alginate and loaded encapsulated bio-molecules by time. Material flow and concentration through mixture chamber is controlled by regulating positive nozzle pressures (P_A and P_B) connected to an air pressure control unit based on the developed formula in [9]. C_A=3% (w/v) and C_B=5% (w/v) sodium alginate solutions were prepared, and 0.3% (w/v) and 0.6% (w/v) micro-glass beads were loaded respectively to represent encapsulated bio-molecules. 1% (w/v) Calcium chloride solution is used to crosslink dispensed sodium alginate. The reader is referred to our earlier work [34] for detail information about the biofabrication process.

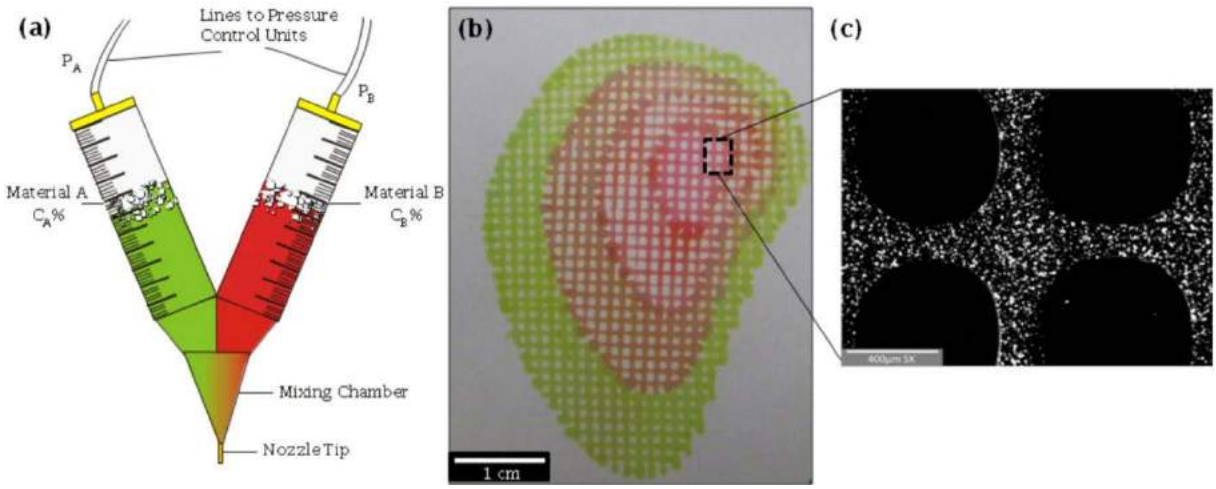

Fig. 10: Biofabrication: (a) NC driven multi-syringe single nozzle dispensing system, (b) fabricated wound scaffold, and (c) micro-scale view loaded with micro-glass beads.

Green and red color inks are incorporated into syringes to represent spatial variation. While ink diffuses through 3D scaffold, only top layer was fabricated for clarification purpose. For complex 3D scaffolds, the reader is referred to our previous work [26]. Fig. 10(b) shows the fabrication of designed model with 4 regions dispensed through 250μm nozzle tip. Distribution of micro-glass beads is demonstrated in Fig. 10(c) on a dark field image taken by 5.0x1.0x1.0 optic lens.

5 CONCLUSION

In this paper, a novel development of porous wound scaffolds is proposed to improve wound healing process. Repair of complex 3-D wound geometry is enhanced by incorporating encapsulated bio-

molecules locally and temporarily based on their interaction with the target cells. A blending process is developed to generate heterogeneous scaffolds using wound features recognized by using imaging study. Hence, 3-D scaffold geometry is partitioned into several uniform regions with varying concentration of bio-molecules and biomaterial. Wound healing can be accelerated by synchronizing the release time of a particular region with the healing time of that region. Multi-syringe single nozzle dispensing system is used to fabricate a sample wound scaffold.

6 ACKNOWLEDGEMENTS

The research was partially funded by U.S. Army Medical Research Grant #: W81XWH-05-1-0401. The authors would like to thank Dr. Robert Hard in the Department of Pathology and Anatomical Sciences at University at Buffalo for micro-scale dark field image.

REFERENCES

[1] Agren, M.: Four alginate dressings in the treatment of partial thickness wounds: a comparative experimental study, British Journal of Plastic Surgery, 49,1996, 129-134.

[2] Albouy, B.; Lucas, Y.; Treuillet, S.: 3d Modeling from uncalibrated color images for a complete wound assessment tool, in Proceedings of the 29th Annual International Conference of the IEEE EMBS Cité Internationale, Lyon, France 2007.

[3] Bell, E.; Ehrlich, H.: Living tissue formed in vitro and accepted as skin-equivalent tissue of full thickness, Science, 211 (4486),1981, 1052-1054. doi:10.1126/science.7008197

[4] Blair, S.; Jarvis, P.; Salmon, M.; McCollum, C.: Clinical trial of calcium alginate haemostatic swabs, British Journal of Plastic Surgery, 77,1990, 568-570.

[5] Bon, F.X.; Briand, E.; Guichard, S.; Couturaud, B.; Revol, M.; Servant, J.M.; Dubertret, L.: Quantitative and kinetic evolution of wound healing through image analysis., IEEE Trans Med Imaging, 19 (7),2000, 767-772. doi:10.1109/42.875206

[6] Cardinal, M.; Eisenbud, D. E.; Amstrong, D. G.: Wound shape geometry measurement predict eventual wound healing, in 18th Annual Meeting of Wound Healing Society, San Diego, CA, 2008.

[7] Chang, R.; Nam, J.; Sun, W.: Computer-Aided Design, Modeling, and Freeform Fabrication of 3D Tissue Constructs for Drug Metabolism Studies, Computer-Aided Design and Application, 5,2008, 21-29.

[8] Chang, R.; Nam, J.; Sun, W.: Direct Cell Writing of 3D Micro-organ for In Vitro Pharmacokinetic Model, Tissue Engineering, 14 (2),2008, 157-169.

[9] Chimate, C.; Koc, B.: Pressure Assisted Multi-syringe Single Nozzle Deposition System for fabrication of Heterogeneous Tissue Scaffolds, in Industrial and Systems EngineeringUniversity at Buffalo, Buffalo, 2010.

[10] Cukjati, D.; Rebersek, S.; Karba, R.; Miklavcic, D.: Modeling of chronic wound healing dynamics, Med. Biol.Eng.Comput., 38,2000, 339-347. doi:10.1007/BF02347056

[11] Curran, M.P.; Plosker, G. L.: Bilayered bioengineered skin substitute (Apligraf): a review of its use in the treatment, BioDrugs, 16 (6),2002, 438-455.

[12] Dow, G.: Bacterial Swabs and the Chronic Wound: When, How, and What Do They Mean, Ostomy Wound Management, 49 (5A),2003, 8-13.

[13] Falanga, V.; Margolis, D.; Alvarez, O.; Auletta, M.; Maggiacomo, F.; Altman, M.; Jensen, J.; Sabolinski, M.; Hardin-Young, J.: Rapid healing of venous ulcers and lack of clinical rejection with an allogeneic cultured human skin equivalent. Human Skin Equivalent Investigators Group, Dermatol, 134 (3),1998, 293-300.

[14] Feedar, J. A.; Kloth, L. C.; Gentzkow, G.D.: Chronic dermal ulcer healing enhanced with monophasic pulsed electrical simulation, Phys. Ther. , 71,1991, 639-649.

[15] Gilman, T.: Parameter for measurement of wound closure, Wounds, 2,1990, 95-101.

[16] Gorin, D.; Cordts, P.; LaMorte, Y.; Menzoian, J.: The influence of wound geometry on the measurement of wound healing rates in clinical trials, J Vas Surg, 23,1996, 524-528.

[17] Griffiths, M.; Ojeh, N.; Livingstone, R.; Price, R.; Navsaria, H.: Survival of Apligraf in Acute Human Wounds, Tissue Engineering, 10 (7-8),2004, 1180-1195.

[18] Hanna, J. R.; Giacopelli, J. A.: A Review of Wound Healing and Wound Dressing Products, The Journal of Foot and Ankle Surgery 36 (1),1997, 2-14. doi:10.1016/S1067-2516(97)80003-8
[19] Hansen, G. L.; Sparrow, E. M.; Kokate, J. Y.; Leland, K. J.; Iaizzo, P.A.: Wound status evaluation using color image processing, IEEE Trans Med Imaging, 16,1997, 78-86. doi:10.1109/42.552057
[20] Helbich, T. H.; Roberts, T. P. L.; Rollins, M. D.; Shames, D.M.;Turetschek, K.;Muhler, H.W.H.M.;Hunt, T.K.;Brasch, R.C.: Noninvasive Assessment of Wound-healing Angiogenesis with Contrast-enhanced MRI1, Acad Radiol 9(suppl 1),2002, S145-S147. doi:10.1016/S1076-6332(03)80423-3
[21] Herbin, M.; Bon, F.X.; Venot, A.; Jeanlouis, F.; Dubertret, M.L.; Strauch, G.: Assessment of healing kinetics through true color image processing, IEEE Trans Med Imaging 12 (1),1993, 39-43.
[22] Johsan, M.: Using cluster analysis to develop a healing typology in vascular ulcers, J. Vasc. Nurs., 15,1997, 45-49. doi:10.1016/S1062-0303(97)90000-5
[23] Juliano, R.L.; Haskell, S.: Signal transduction from the extracellular matrix, J Cell Biol 120,1993, 557-585. doi:10.1083/jcb.120.3.577
[24] Kale, S.: Feature-Based Bio-mimetic Modeling of Heterogenous Scaffolds for Imroved Tissue Engineering, in Industrial and Systems Engineering Department,University at Buffalo, Buffalo, 2009.
[25] Khalil, S.; Sun, W.: Biopolymer deposition for freeform fabrication of hydrogel tissue constructs, Material Science and Engineering: C, 27 (3),2007, 469-478. doi:10.1016/j.msec.2006.05.023
[26] Khoda, A.; Ozbolat, I.; Koc, B.: Engineered Tissue Scaffolds with variational porosity architecture, in Journal of Biomechanical Engineering (In Press), 2010.
[27] Kloppenberg, F.W.H.; Beerthuizen, G.I.J.M.; Duis, H.J.t.: Perfusion of burn wounds assessed by Laser Doppler Imaging is related to burn depth and healing time, Burns, 27,2001, 359-363.
[28] Knill, C.; Kennedy, K.; Mistry, J.; Miraftab, M.; Smart, G.;Groocock, M.;Williams, H.: Alginate fibres modified with unhydrolysed and hydrolysed chitosans for wound dressings, Polymers, 55,2004, 65-76.
[29] Lanza, R.; Langer, R.;Vacanti, J.: Principles of Tissue Engineering, Elsevier,2007.
[30] Liu, J.; Bowyer, K.; Goldgof, D.; Sarkar, S.: Acomparative study of textures measures for human skin treatment,Proceedings of International Conference on Information, Communication Signal Processing ICICS, Beijing, China,1997.
[31] Manaker, G.M.: Wound Dressing in the new Millennium, Seminars in Cutaneous Medicine and Surgery, 21 (2),2002, 171-175. doi:10.1053/sder.2002.33287
[32] Manios, A.;Tosca, A.;Volakakis, E.;Leivadara, M.;Tsiftsis, D.: Computer assisted evaluation of wound healing in chronic ulcers, Computers in Biology and Medicine, 33,2003, 311-317.
[33] Martin, P.: Wound Healing-Aiming for Perfect Skin Regeneration, Science, 276 (5309),1997, 75-81.
[34] Ozbolat, I.T.; Koc, B.: Modeling of Spatially Controlled Bio-molecules in Three-dimensional Porous Alginate Structures ASME transactions, J of Medical Devices, 4(4),2010, 041003(1)-041003(11).
[35] Ozbolat, I.T.; Koc, B.: Spatially controlled biomolecules in 3D porous structures,Industrial Engineering Research Conference, Cancun, Mexico,2010.
[36] Ozbolat, I.T.; Marchany, M.; Bright, F.V.; Cartwright, A.N.; Gardella, J.A.; Hard, R.; Hicks, W.L.; Koc, B.: Feature Based Bio-Modeling of Micro-patterned Structures for Tissue Engineering, Computer-Aided Design and Applications, 6 (5),2009, 661-671.
[37] Pereira, C.; Gold, W.; Herndon, D.: Review Paper: Burn Coverage Technologies: Current Concepts and Future Directions, Journal of Biomaterials Applications, 22,2007, 101-121.
[38] Perkins, J.; Desai, S.; Harrison, B.; Sankar, J.: Understanding Release Kinetics of Calcium Alginate Microcapsules Using Drop on Demand Inkjet Printing, in ASME International Mechanical Engineering Congress & Exposition, FL, 2009.
[39] Pettet, G.J.; Bryne, H.M.; Mcelwain, D.L.S.; Norbury, J.: A Model of Wound Healing Angiogenesis in Soft Tissue, Mathematical Biosciences, 136,1995, 35-63. doi:10.1016/0025-5564(96)00044-2
[40] Putney, S.D.;Burke, P.A.: Improve protein therapeutics with sustained release formulations, Nature Biotecnol., 16,1998, 153-157. doi:10.1038/nbt0298-153
[41] Ribeiro, C.; Barrias, C.; Barbosa, M.: Calcium phosphate-alginate microspheres as enzyme delivery matrices, Biomaterials, 25 (18),2004, 4363-4373. doi:10.1016/j.biomaterials.2003.11.028
[42] RobertMcNeel&Associates: Rhinoceros 4.0, Seattle, 2007.

[43] Sachlos, E.; Czernuszka, J.T.: Making Tissue Engineering Scaffolds Work: Review on the application of solid freeform fabrication technology to the production of tissue engineering scaffolds, European Cells and Materials, 5,2003, 29-40.
[44] Samanta, K.; Koc, B.: Feature-based design and material blending for free-form heterogeneous object modeling, Computer-Aided Design, 37 (3),2005, 287-305. doi:10.1016/j.cad.2004.03.005
[45] Samanta, K.; Koc, B.: Feature-based material blending for heterogeneous object modeling, Heterogeneous Objects Modeling and Applications Heidelberg: Springer Berlin,2008, 142-166.
[46] Savakis, A.E.; Maggelakis, S.A.: Models of Shrinking Clusters with Applications to Epidermal Wound Healing, Mathl. Comput. Modelin, 25,1997, 1-6. doi:10.1016/S0895-7177(97)00034-4
[47] Sheardown, H.; Cheng, Y.-L.: Mechanism of Corneal Epithelial Wound Healing, Chemical Engineering Science, 51 (19),1995, 4517-4529. doi:10.1016/0009-2509(96)00299-0
[48] Sherratt, J.A.; Dallon, C.D.: Theoretical models of wound healing: past success and future challenges, C.R. Biologies, 325,2002, 557-564. doi:10.1016/S1631-0691(02)01464-6
[49] Stashak, T.S.; Farstvedt, E.; Othic, A.: Update on Wound Dressings: Indications and Best Use, Clinical Techniques in Equine Practice, Clin Tech Equine Pract 3,2004, 148-163.
[50] Stefanovska, A.; Vodovnik, L.; Benko, H.; Turk, R.: Treatment of chronic wounds by means of electric and electro-magnetic fields, Part 2 Values of FES parameters for pressure score treatment, Med. Biol. Eng. Comput., 31,1993, 213-220. doi:10.1007/BF02458039
[51] Tallman, P.; Muscare, E.; Carson, P.; Eaglstein, W.H.; Falanga, V.: Initial rate of healing predicts complete healing of venous leg ulcers, Arch Dermatol 133,1997, 1231-1324.
[52] Tranquillo, R.T.; Murray, J.D.: Mechanistic Model of Wound Contraction, Journal of Surgical Research, 55,1993, 233-247. doi:10.1006/jsre.1993.1135
[53] Winter, G.: Formation of the scab and the rate of epithelialization of superficial wounds in the skin of the young domestic pig, Nature 193,1962, 293-294. doi:10.1038/193293a0
[54] Yushkevich, P.A.; Piven, J.; Hazlett, H.C.; Smith, R.G.; Ho, S.; Gee, J.C.; Geri, G.: User-guided 3D active contour segmentation of anatomical structures: Significantly improved efficiency and reliability, NeuroImage, 31,2006, 1116-1128. doi:10.1016/j.neuroimage.2006.01.015